Supplementary Information

Long-lived electrets and lack of ferroelectricity in methylammonium lead bromide $CH_3NH_3PbBr_3$ ferroelastic single crystals

Alessandra Geddo Lehmann[a], Francesco Congiu[*a], Daniela Marongiu[a], Andrea Mura[a], Alessio Filippetti[a,b], Alessandro Mattoni[*b], Michele Saba[a], Guido Pegna[a], Valerio Sarritzu[a], Francesco Quochi[a] and Giovanni Bongiovanni[a]

[a]Dipartimento di Fisica, Università degli Studi di Cagliari, I-09042 Monserrato (CA), Italy

[b]Istituto Officina dei Materiali, CNR-IOM SLACS Cagliari, Cittadella Universitaria, I-09042 Monserrato (CA), Italy

[*] franco.congiu@dsf.unica.it, mattoni@iom.cnr.it
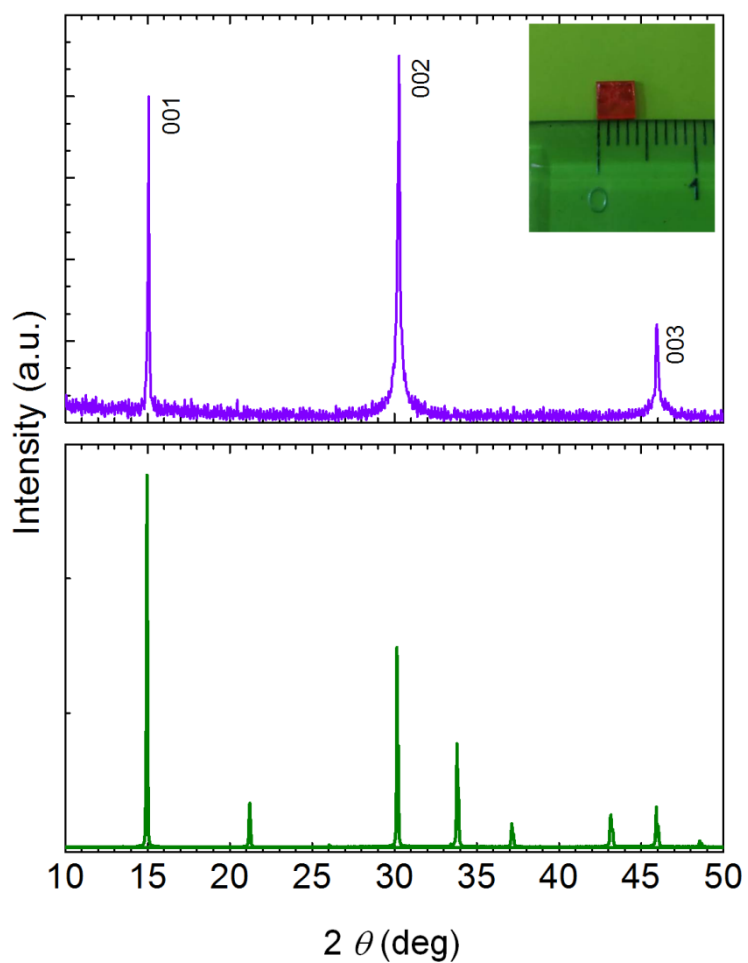
SI 1. X-ray diffraction characterization

Fig. S1 (a) Specular X-ray diffraction from a MAPB crystal surface, confirming the $(100)_{cub}$ crystallographic orientation, which is consistent with the rectangular morphology of the $\{100\}_{cub}$ as-grown faces (inset). **(b)** Powder diffraction pattern of a grinded single crystal.
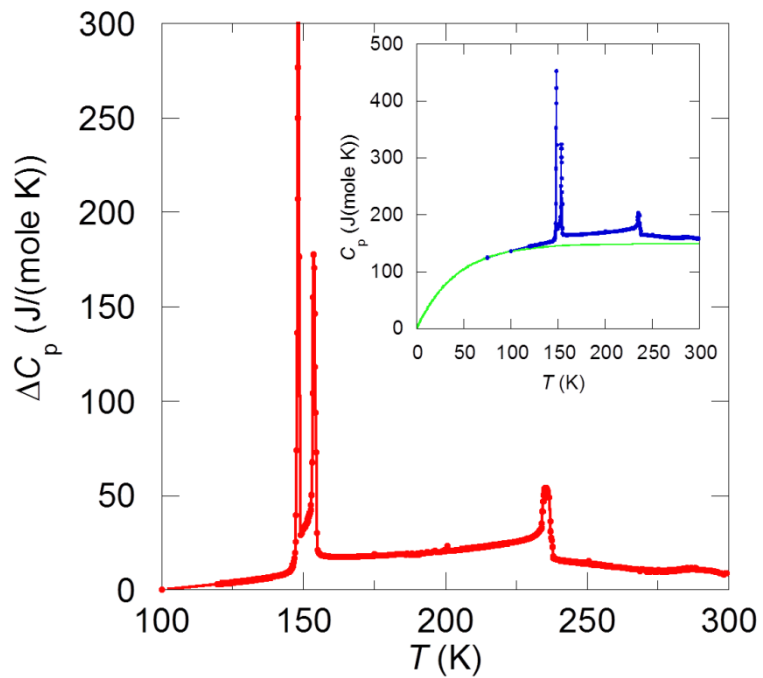
SI 2. Specific heat measurement.

Fig. S2. Specific heat C_p measured on cooling on a small MAPB sample (a single crystal fragment of 14 mg). Data were analyzed according to the method proposed in Ref.[1] in order to obtain the excess (transitional) component ΔC_p as the difference between the measured C_p values (Inset, blue curve) and the normal part (Inset, green curve). Three main anomalies are visible, representing the three reversible phase transitions related to the cubic $\rightarrow$ tetragonal $\rightarrow$ intermediate tetragonal $\rightarrow$ orthorhombic symmetry breaking.
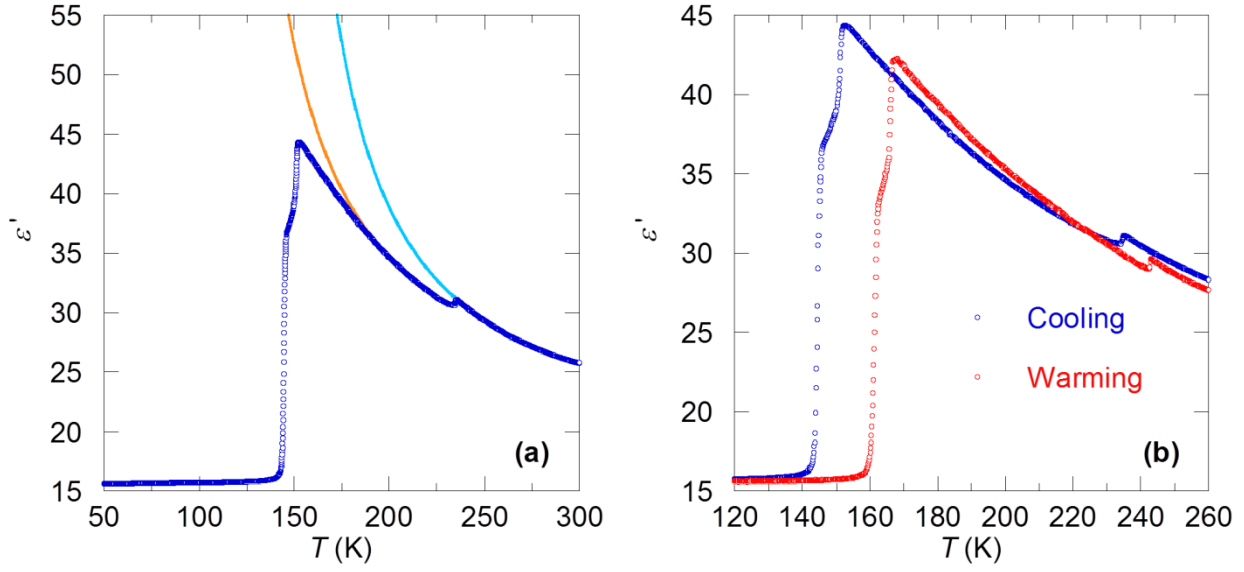
SI 3. Dielectric constant measurement.

Fig. S3. (a) Real part of the dielectric permittivity $\varepsilon'(T)$ of MAPB, measured on cooling (2.0 K/min) through the phase transitions one of the single crystals used in this work, for frequency of 1 MHz. In agreement with the literature[2] at the measuring frequency of 1 MHz the dielectric constant in the cubic and tetragonal phases is mainly ascribed to the fast process of orientational polarization of the almost free MA$^+$ permanent electric dipoles and it is well represented by a Curie-Weiss law:

$$\varepsilon'(T) = A + \frac{C}{T-\theta} \tag{1}$$

which describes a paraelectric state[3]. In (1), A is the asymptotic value of $\varepsilon'(T)$ at high temperature, C is the Curie constant, T is the absolute temperature, θ is a phenomenological parameter that takes into account any kind of correlated motion of dipoles. The disordered to ordered state of MA$^+$ dipoles at the transition to the orthorhombic phase is signed by the jump of the dielectric constant and the concomitant disappearance of the Curie-Weiss behavior[4]. The existence of the intermediate phase is well visible in the double jump at about 152 K. The light blue continuous curve and the orange one show the Curie-Weiss fit to Eq. (1) for the cubic and tetragonal phase, respectively. Fitting parameters A, the Curie constant C and the Curie-Weiss temperature θ are reported in Table I.

(b) Thermal hysteresis of ε' measured at 1 MHz frequency on cooling (blue) and on warming (red). A significant thermal hysteresis of about 15 K between $\varepsilon'(T)$ values measured on cooling and on warming can be observed, which is a clear indication of the first order character of the tetragonal to orthorhombic phase transition. For the cubic to tetragonal phase transition a smaller hysteresis of about 9 K is observed.

MAPB	θ (K)	A	C (K)	ΔT fit (K)
Cubic	136	17	1417	255 ÷ 275
Tetragonal	106	19	1507	196 ÷ 233

Table I. Fitting parameters to the Curie Weiss law for $\varepsilon'(T)$ at 1 MHz measured on cooling
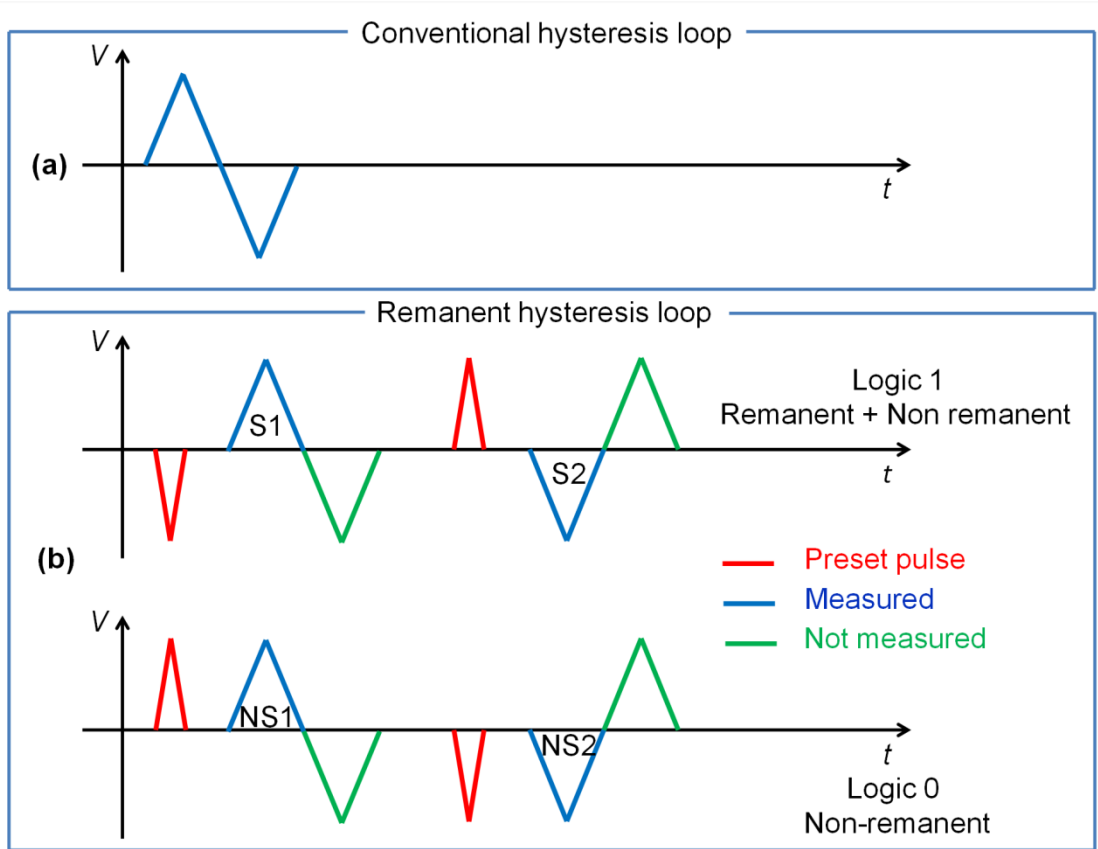
SI 4. Remanent hysteresis measurements.

Fig. S4. Schematic of the voltage pulse profile used in conventional hysteresis loop measurements **(a)** and in remanent hysteresis measurements **(b)**.

Remanent polarization is the polarization that remains in a material after the removal of the applied field. Conventional $P(E)$ loops, typically obtained by applying a bipolar triangular voltage pulse (**Fig. S4a)**), show the total sample response to the stimulus voltage. This response contains both hysteretic (denoted as true remanent, or switchable, or intrinsic) and non-hysteretic (non-remanent) contributions. True remanent polarization is the polarization of most interest, as it maintains its state once switched. Non-remanent polarization also "switches" with the remanent (i.e. it follows the electric field) but, once the applied field is removed, it does not maintain its switched state, but rather randomizes. These two contributions can be separated by means of the "Remanent Polarization" measuring task performed by the Vision software driving the Radiant Tester. This task is composed by two "logics" named Logic 1 and Logic 0 (**Fig. S4b**). Both logics are formed by two hysteresis measurements; each of them is preceded by a preset pulse. In Logic 1, both the legs of the triangular bipolar field pulse S1 and S2, during which polarization is measured, switch the polarization state of the sample. Logic 1 therefore measures both remanent and non-remanent polarization. During Logic 0 only the non-remanent polarization is measured since neither leg (NS1 and NS2) of the triangular bipolar pulse causes polarization switching. Thus, subtraction of Logic 0 (non-remanent) measurement from Logic 1 (remanent plus non-remanent) measurement gives as a result the true remanent polarization vs applied electric field $P_R(E)$ loop[5,6].

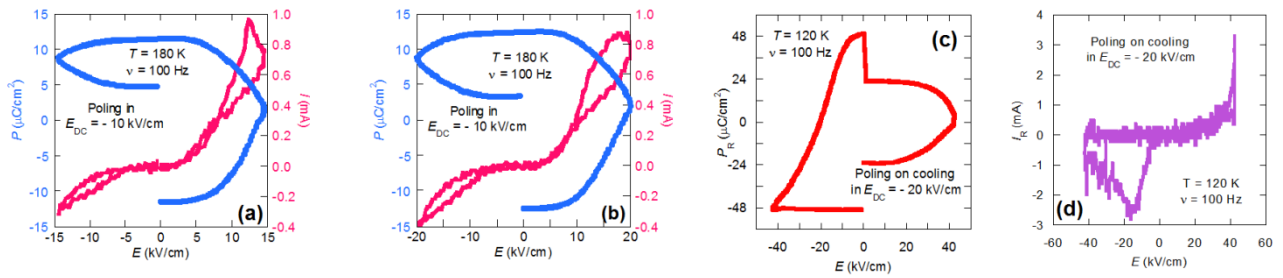## SI 5. Poling of T-MAPB and O-MAPB in negative fields

Figure S5. Poled crystals. **(a)** and **(b)** $P(E)$ and $I(E)$ loops of T-MAPB after poling in an electric field E_{DC} = -10 kV/cm, for two values of the measuring E_{AC} field.; in **(a)**, a weak switching current is observed in the low-resistance $I(E)$ branch, however embedded in a large resistive type leakage current. **(c)** Remanent polarization loop $P_R(E)$ of O-MAPB cooled from 180 K in E_{DC} = -20 kV/cm and **(d)** corresponding current loop $I_R(E)$, showing the resistive switching peak in the negative E_{AC} quadrant.

References

1   N. Onoda-Yamamuro, T. Matsuo and H. Suga, *J. Phys. Chem. Solids*, 1990, **51**, 1383–1395.

2   N. Onoda-Yamamuro, T. Matsuo and H. Suga, *J. Phys. Chem. Solids*, 1992, **53**, 935–939.

3   G. Rupprecht and R. O. Bell, *Phys. Rev.*, 1964, **135**, A748–A752.

4   A. Mattoni and C. Caddeo, *J. Chem. Phys.*, 2020, **152**, 104705.

5   A. J. Joseph, S. Goel, A. Hussain and B. Kumar, *Ceram. Int.*, 2017, **43**, 16676–16683.

6   H. J. Lee, C. W. Ahn, S. S. Won, A. Tange, B. C. Park, H. J. Seog and I. W. Kim, *J. Korean Phys. Soc.*, 2015, **66**, 1401–1405.